

VIP Very Important Paper

Weak σ -Hole Triel Bond between C_5H_5Tr ($Tr = B, Al, Ga$) and Haloethyne: Substituent and Cooperativity EffectsQingqing Yang,^[a] Bohua Zhou,^[a] Qingzhong Li,^{*[a]} and Steve Scheiner^{*[b]}

The replacement of a CH group of benzene by a triel (Tr) atom places a positive region of electrostatic potential near the Tr atom in the plane of the aromatic ring. This σ -hole can interact with an X lone pair of XCCH (X=F, Cl, Br, and I) to form a triel bond (TrB). The interaction energy between C_5H_5Tr and FCCH lies in the range between 2.2 and 4.4 kcal/mol, in the order $Tr=B < Ga < Al$. This bond is strengthened by halogen substituents on the ring, particularly on the site adjacent to Tr. There is

a much stronger strengthening trend as the F of the FCCH nucleophile is replaced by the heavier halogen atoms, rising up to 22 kcal/mol for ICCH. Adding a Li^+ cation above the ring pulls density toward itself and thus magnifies the Tr σ -hole. The TrB to the XCCH nucleophile is thereby magnified as is the strength of the TrB. This positive cooperativity is particularly large for $Tr=B$.

1. Introduction

The triel bond (TrB) is a novel and intriguing intermolecular force, defined as an interaction between a Group III atom and an electron donor.^[1] Owing to the electron deficiency of boron, the lightest member of this family, its compounds and complexes typically act as a Lewis acid, which can bind with a Lewis base, as in BF_3-HCN and BF_3-NH_3 .^[2-4] The electron deficiency of boron is usually attributed to the presence of an empty p orbital in the sp^2 -hybridized boron molecule. This electron configuration also has an impact on the surrounding molecular electrostatic potential (MEP). There are two positive MEP regions, above and below the molecular plane of BF_3 and BCl_3 , which are commonly denoted π -holes.^[5] Of course, such π -holes are not unique to B, but arise also around the N atom of $-NO_2$ and the C atom of $-C=O$.^[5] These π -holes are actually less common in a general sense than the σ -hole that is situated along the extension of a covalent bond,^[6] quite often for Group IV–VII atoms. However, the presence of σ -hole is quite uncommon for a group III atom,^[7,8] for reasons explained above. There are exceptions though. For example, the π -hole in BH_3 can be changed into a σ -hole in the context of the BH_3 dimer.^[8]

Although the TrB is fairly new to chemical thinking, its applications in chemical reactions have already begun to be explored.^[9-13] Triethylamine is a scavenger of borine (BH_3) by a S_N2 bond activation can be promoted if electron-rich iridium(I) and palladium(0) attack the B atom through a S_N2 -

type oxidative addition pathway.^[11] In the S_N2 reaction, a pentacoordinate boron compound is formed and this compound, with a hypervalent boron center, can be isolated.^[12] A TrB is also of importance in the H_2 release from ammonia-borane.^[13] Metal-free catalysis is sometimes realized by using sterically encumbered Lewis acid–base pairs, in which B serves as a Lewis acid center.^[14] Besides the applications in chemical reactions, the unique electrophile property of boron determines its chameleonic ability to engage protein targets.^[15] These and other applications have led to more scrutiny of TrBs recently.^[16-20]

Boron has a strong affinity for an electron donor, with an interaction energy as high as 90 kcal/mol.^[17] This strong interaction is often accompanied by a prominent distortion from a planar structure to an umbrella-like pyramid.^[17] This large distortion is an important ingredient in the TrB, and can complicate the analysis of the roles of electrostatic, polarization, and dispersion in TrB formation. This large distortion is also responsible for some abnormal variations in TrBs. For example, BF_3 contains a deeper π -hole than BH_3 , yet engages in a weaker TrB due to the smaller deformation in the BF_3 complex.^[21] As another issue, it is recognized that organic fluorine is a poor electron donor in hydrogen bonds,^[22] which raises the question as to whether this would also be true in TrBs.

Along the line of HBs, although the TrB has certain different properties, it is the similarities that are most striking. Charge density shifts from the Lewis base to the acid in both types of interactions.^[23] Electron-donating substituents on the Lewis base have an enhancing effect, while those in the acid show an opposite effect.^[24] The strength of both are affected by solvent and hybridization.^[25] Like the HB, the TrB becomes stronger if the group adjoining the triel atom is positively charged.^[26] Several theoretical studies have probed the cooperativity of the TrB with other types of interactions including the hydrogen,^[27] halogen,^[28] chalcogen,^[29] pnictogen,^[30] and tetrel bond,^[31] cation- π interaction,^[32] anion- π interaction,^[33] and regium bond.^[34] As one example, cations bound to the phenyl ring of $PhBH_3$ substantially deepens the π -hole on B and well as the TrB

[a] Dr. Q. Yang, B. Zhou, Q. Li
Laboratory of Theoretical and Computational Chemistry and School of Chemistry and Chemical Engineering, Yantai University
264005 Yantai (China)
E-mail: li70316@sohu.com

[b] Prof. S. Scheiner
Department of Chemistry and Biochemistry, Utah State University
84322-0300 Logan, UT (USA)
E-mail: steve.scheiner@usu.edu

Supporting information for this article is available on the WWW under <https://doi.org/10.1002/cphc.202000955>

strength, and shortens the B...N distance by an amount that depends on the nature of the cation.^[32] The triel bond examined in these cooperative effects arises from a π -hole interaction. There is however some earlier study of cooperativity involving a σ -hole triel bond, in the context of $C_5H_5B\cdots NCX\cdots NCY$ ($X=F, Cl, Br, I; Y=H, CN, OH, Li$), where a triel bond and a halogen bond coexist.^[7] Interestingly, the σ -hole triel bond is weakened by the halogen bond.^[7]

It is clear that the triel bond warrants more detailed study. There are some outstanding questions which merit some examination. In the first place, how is the TrB affected if the Tr atom is placed within the confines of an aromatic ring? This bonding situation leaves a vacant sp^2 orbital as the source of a positive region of MEP, a σ -hole of sorts, in the plane of the aromatic system. To add to the novelty, unlike the typical σ -hole, this one does not lie along the extension of any covalent bond, but rather along a bisector. This situation is modeled here by the C_5H_5Tr molecule in which Tr refers to B, Al, and Ga. Another question concerns the manner in which substitution at various sites on the phenyl ring might affect the TrB in which this aromatic system is engaged. Moreover, due to the rigidity of the ring, only minimal geometric distortions are anticipated upon complexation, so this system ought to be able to avoid the complicating effects of deformation energy. As electron donors, the alkynes $XC\equiv CH$ are considered where X refers to one of several halogen atoms. The C sp -hybridization of these systems can be supposed to make them rather weak donors, so ought to serve as a stringent test of the ability of the Tr atoms to engage in noncovalent $Tr\cdots X$ bonding. The comparisons should also shed light on how electronegativity and polarizability of the bonding X atom affects the nature of the TrB. As a final refinement, a Li^+ cation is placed above the aromatic ring, and its effects upon the TrB is assessed. In particular, this third entity allows an evaluation of the cooperativity between the TrB and a cation- π interaction.

Computational Methods

All calculations were carried out at the MP2/aug-cc-pVTZ level using the Gaussian09 software.^[35] To confirm that optimized structures are true minima, no imaginary frequencies were found. For binary systems, both interaction energy (E_{int}) and binding energy (E_b) represent the difference between the energy of the complex and the sum of monomer energies, where they adopted the structures within the complex, and their fully optimized ones, respectively. The difference between E_{int} and E_b is termed the deformation energy (DE). Both quantities were corrected for the basis set superposition error (BSSE) using the Boys and Bernardi counterpoise method.^[36]

The wavefunction calculated at the MP2/aug-cc-pVTZ level was used to obtain molecular electrostatic potentials (MEPs) on the 0.001 au isodensity surface using the WFA-SAS program.^[37] Topological parameters including electron density (ρ), Laplacian ($\nabla^2\rho$), and energy density (H) at the bond critical point (BCP) were analyzed using AIM2000 software.^[38] NBO analysis was performed at the HF/aug-cc-pVTZ level via the NBO3.0 program^[39] in the Gaussian09 package to obtain charge transfer

and interorbital interactions. The localized molecular orbital energy decomposition analysis (LMOEDA)^[40] method in the GAMESS program^[41] was used to decompose the interaction energy at the MP2/aug-cc-pVTZ level into five physically significant components: electrostatic energy (E^{ele}), exchange energy (E^{ex}), repulsion energy (E^{rep}), polarization energy (E^{pol}) and dispersion energy (E^{disp}).

2. Results

2.1. Monomers

The molecular electrostatic potentials (MEPs) of the various Tr derivatives of benzene are displayed in Figure 1, where they are each labeled as Trz where Tr refers to the particular triel atom. The most conspicuous feature of each diagram is the red region of positive MEP close to the Tr atom, and centered in the molecular plane. Each such region is referred to here as a σ -hole, although it differs from most such holes in that it does not lie directly opposite any one particular covalent bond, but rather bisects a pair of $Tr-C$ bonds. The most positive region is connected with Alz, followed in order by Gaz and then Bz, which is consistent with the Tr electronegativity. The MEPs of the various $XC\equiv CH$ molecules are depicted in Figure 2. Each contains a red positive area near the H atom, but the most pertinent section with respect to complexation with the benzene derivatives is the negative region near the halogen atom. The minimum in the MEP lies somewhat off of the molecular axis, where one might expect the lone pairs of the X atom to be situated. The magnitude of this minimum is fairly shallow, less than -0.006 au. Its value is opposite to the electronegativity order, most intense for $X=I$, and least for Cl and F.

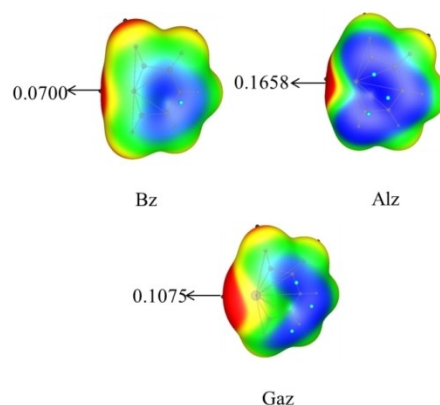


Figure 1. MEP on the 0.001 au isodensity surface of the Trz monomers. Color ranges, in au, are: Red, >0.02 ; yellow, $0.02-0$; green, $0-0.02$; blue, <-0.02 .

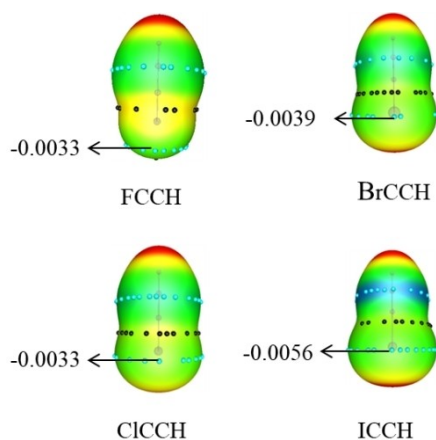


Figure 2. MEP on the 0.001 au isodensity surface of the $\text{XC}\equiv\text{CH}$ monomers. Color ranges are the same as those in Figure 1.

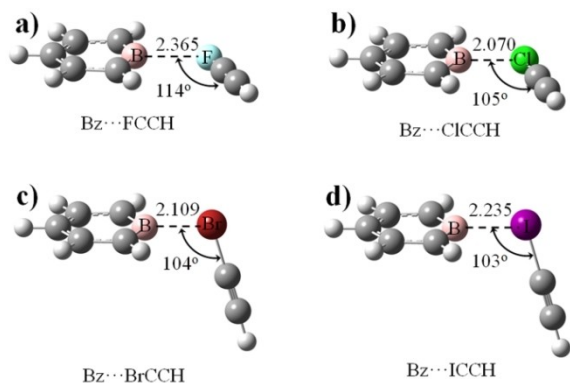


Figure 3. Optimized structures of $\text{Bz}\cdots\text{XCCH}$ dimers. Distances in Å and angles in degs.

Table 1. $\text{Tr}\cdots\text{X}$ distance (R , Å), interaction energy (E_{int} , kcal/mol), binding energy (E_{b} , kcal/mol), and deformation energy (DE , kcal/mol) in the binary systems.

| | R | E_{int} | E_{b} | DE |
|---|-------|------------------|----------------|------|
| $\text{Bz}\cdots\text{FCCH}$ | 2.365 | -2.15 | -2.03 | 0.12 |
| $\text{Bz}\cdots\text{ClCCH}$ | 2.070 | -12.39 | -7.68 | 4.71 |
| $\text{Bz}\cdots\text{BrCCH}$ | 2.109 | -16.95 | -9.92 | 7.03 |
| $\text{Bz}\cdots\text{ICCH}$ | 2.235 | -21.98 | -13.40 | 8.58 |
| $\text{Alz}\cdots\text{FCCH}$ | 2.229 | -4.41 | -3.86 | 0.55 |
| $\text{Gaz}\cdots\text{FCCH}$ | 2.426 | -2.25 | -2.00 | 0.25 |
| $\gamma\text{-F-Bz}\cdots\text{FCCH}$ | 2.197 | -2.76 | -2.42 | 0.34 |
| $\beta\text{-F-Bz}\cdots\text{FCCH}$ | 2.214 | -2.65 | -2.33 | 0.32 |
| $\alpha\text{-F-Bz}\cdots\text{FCCH}$ | 1.924 | -4.60 | -3.10 | 1.50 |
| $\alpha\text{-Cl-Bz}\cdots\text{FCCH}$ | 1.967 | -4.37 | -3.10 | 1.27 |
| $\alpha\text{-Br-Bz}\cdots\text{FCCH}$ | 1.973 | -4.29 | -3.06 | 1.23 |
| $\alpha\text{-F-Alz}\cdots\text{FCCH}$ | 2.281 | -4.41 | -3.85 | 0.56 |
| $\alpha\text{-Cl-Alz}\cdots\text{FCCH}$ | 2.258 | -5.02 | -4.42 | 0.60 |
| $\alpha\text{-Br-Alz}\cdots\text{FCCH}$ | 2.251 | -5.21 | -4.58 | 0.63 |
| $\alpha\text{-F-Gaz}\cdots\text{FCCH}$ | 2.404 | -2.41 | -2.09 | 0.32 |
| $\alpha\text{-Cl-Gaz}\cdots\text{FCCH}$ | 2.398 | -2.89 | -2.54 | 0.35 |
| $\alpha\text{-Br-Gaz}\cdots\text{FCCH}$ | 2.336 | -2.92 | -1.71 | 1.21 |

2.2. Complexes with Bz

The optimized geometries of the complexes of Bz with XCCH are illustrated in Figure 3. The $R(\text{B}\cdots\text{X})$ distance is rather long at 2.365 Å for $\text{X}=\text{F}$, with the intermolecular distance in the other three complexes all less than 2.3 Å, and follow the order commensurate with the size of the X atom: $\text{Cl} < \text{Br} < \text{I}$. There is also a trend of gradually diminishing $\theta(\text{B}\cdots\text{XC})$ angle for larger X, which can be understood by means of MEP maps of XCCH in Figure 2. The location of the most negative MEP on the X atom is different and gradually deviates from the molecular axis for the heavier X atom. The energetics of the complexes are compiled in Table 1 agree with the intermolecular distances in that the dimer with FCCH is most weakly bound. The interaction energies of the other three complexes vary from 12 to 22 kcal/mol, and rise along with the size of the X atom. The latter trend agrees with the more intense MEP minima in Figure 2 for larger X. There is also a tendency toward greater deformation energy in the same order, which represents a growing discrepancy between E_{int} and E_{b} .

The relative strengths of these bonds are echoed by the properties of the AIM bond critical point reported in Table 2. The density follows the order $\text{F} \ll \text{Cl} < \text{Br} < \text{I}$, and H becomes progressively more negative in this same order. These negative quantities are suggestive of a small covalent character, although the small densities and positive $\nabla^2\rho$ argue for noncovalency. Measures of charge transfer in these complexes are contained in Table 3. CT refers to the total amount of charge transferred from the XCCH electron donor molecule to Bz, as assessed by natural atomic charges. This quantity is rather large, up to as much as 0.5 e. It also follows the same $\text{F} \ll \text{Cl} < \text{Br} < \text{I}$ pattern as the other indicators above. The bulk of this transfer is attributed to that originating in the X lone pairs and moving over to the NBO orbital designated as an antibonding lone pair on B, labeled Lp^* in NBO terminology. The second-order energetic manifestation of this interorbital transfer $E^{(2)}$ is very large for several of these complexes. Indeed, the interaction is so strong in

Table 2. Electron density (ρ), its Laplacian ($\nabla^2\rho$), and energy density (H) at the $\text{Tr}\cdots\text{X}$ BCP in the binary systems, all in au.

| | ρ | $\nabla^2\rho$ | H |
|---|--------|----------------|---------|
| $\text{Bz}\cdots\text{FCCH}$ | 0.0137 | 0.0528 | 0.0008 |
| $\text{Bz}\cdots\text{ClCCH}$ | 0.0540 | 0.2317 | -0.0282 |
| $\text{Bz}\cdots\text{BrCCH}$ | 0.0650 | 0.2171 | -0.0402 |
| $\text{Bz}\cdots\text{ICCH}$ | 0.0712 | 0.1322 | -0.0508 |
| $\text{Alz}\cdots\text{FCCH}$ | 0.0186 | 0.1090 | 0.0034 |
| $\text{Gaz}\cdots\text{FCCH}$ | 0.0196 | 0.1001 | 0.0021 |
| $\gamma\text{-F-Bz}\cdots\text{FCCH}$ | 0.0187 | 0.0684 | -0.0003 |
| $\beta\text{-F-Bz}\cdots\text{FCCH}$ | 0.0184 | 0.0659 | -0.0002 |
| $\alpha\text{-F-Bz}\cdots\text{FCCH}$ | 0.0299 | 0.1641 | -0.0102 |
| $\alpha\text{-Cl-Bz}\cdots\text{FCCH}$ | 0.0279 | 0.1221 | -0.0097 |
| $\alpha\text{-Br-Bz}\cdots\text{FCCH}$ | 0.0277 | 0.1000 | -0.0091 |
| $\alpha\text{-F-Alz}\cdots\text{FCCH}$ | 0.0164 | 0.0890 | 0.0024 |
| $\alpha\text{-Cl-Alz}\cdots\text{FCCH}$ | 0.0174 | 0.0986 | 0.0029 |
| $\alpha\text{-Br-Alz}\cdots\text{FCCH}$ | 0.0044 | 0.0165 | 0.0010 |
| $\alpha\text{-F-Gaz}\cdots\text{FCCH}$ | 0.0204 | 0.1093 | 0.0026 |
| $\alpha\text{-Cl-Gaz}\cdots\text{FCCH}$ | 0.0209 | 0.1107 | 0.0026 |
| $\alpha\text{-Br-Gaz}\cdots\text{FCCH}$ | 0.0242 | 0.1312 | 0.0020 |

Table 3. NBO charge transfer (CT, e) and second-order perturbation energy ($E^{(2)}$, kcal/mol) in the binary systems.

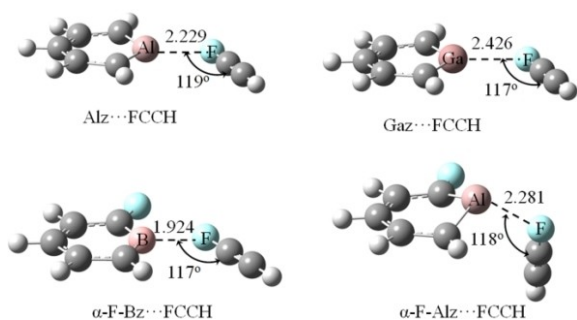
| CT | | $E^{(2)}$ | |
|-----------------|--------|-----------|--------|
| Bz...FCCH | 0.0360 | LpF→Lp*B | 25.76 |
| Bz...ClCCH | 0.3213 | LpCl→Lp*B | 284.65 |
| Bz...BrCCH | 0.4037 | LpBr→Lp*B | 422.27 |
| Bz...ICCH | 0.5025 | LpI→Lp*B | – |
| Alz...FCCH | 0.0582 | LpF→Lp*Al | 44.38 |
| Gaz...FCCH | 0.0409 | LpF→Lp*Ga | 27.44 |
| γ-F-Bz...FCCH | 0.0530 | LpF→Lp*B | 42.25 |
| β-F-Bz...FCCH | 0.0510 | LpF→Lp*B | 40.28 |
| α-F-Bz...FCCH | 0.0994 | LpF→Lp*B | 90.41 |
| α-Cl-Bz...FCCH | 0.0907 | LpF→Lp*B | 80.98 |
| α-Br-Bz...FCCH | 0.0931 | LpF→Lp*B | 80.40 |
| α-F-Alz...FCCH | 0.0482 | LpF→Lp*Al | 37.07 |
| α-Cl-Alz...FCCH | 0.0509 | LpF→Lp*Al | 39.31 |
| α-Br-Alz...FCCH | 0.0515 | LpF→Lp*Al | 39.87 |
| α-F-Gaz...FCCH | 0.0377 | LpF→Lp*Ga | 26.47 |
| α-Cl-Gaz...FCCH | 0.0388 | LpF→Lp*Ga | 30.97 |
| α-Br-Gaz...FCCH | 0.0493 | LpF→Lp*Ga | 35.39 |

Bz...ICCH that NBO deems the complex to be a single covalently bound unit.

Decomposition of the total interaction energies in Table 4 reveals first that exchange energy is the single largest attractive component. Among the others, polarization energy is largest,

Table 4. Electrostatic (E^{ele}), exchange (E^{ex}), repulsion (E^{rep}), polarization (E^{pol}), and dispersion (E^{disp}) energies in the binary systems. All in kcal/mol.

| | E^{ele} | E^{ex} | E^{rep} | E^{pol} | E^{disp} |
|-----------------|------------------|-----------------|------------------|------------------|-------------------|
| Bz...FCCH | −3.11 | −8.53 | 15.28 | −2.14 | −3.68 |
| Bz...ClCCH | −21.96 | −61.61 | 117.90 | −34.92 | −12.34 |
| Bz...BrCCH | −27.30 | −75.72 | 145.83 | −45.97 | −14.01 |
| Bz...ICCH | −29.32 | −86.55 | 164.61 | −54.64 | −16.30 |
| Alz...FCCH | −8.05 | −14.95 | 29.22 | −9.37 | −1.41 |
| Gaz...FCCH | −5.06 | −10.63 | 20.11 | −4.65 | −2.03 |
| γ-F-Bz...FCCH | −4.88 | −12.69 | 23.30 | −4.13 | −4.40 |
| β-F-Bz...FCCH | −4.67 | −12.09 | 22.22 | −3.96 | −4.18 |
| α-F-Bz...FCCH | −10.37 | −25.33 | 48.72 | −11.85 | −5.88 |
| α-Cl-Bz...FCCH | −9.21 | −23.09 | 44.01 | −10.13 | −6.04 |
| α-Br-Bz...FCCH | −9.18 | −23.14 | 44.04 | −9.98 | −6.11 |
| α-F-Alz...FCCH | −7.72 | −16.42 | 31.37 | −8.41 | −3.30 |
| α-Cl-Alz...FCCH | −8.09 | −17.67 | 33.41 | −9.13 | −3.65 |
| α-Br-Alz...FCCH | −8.36 | −18.58 | 34.90 | −9.37 | −3.90 |
| α-F-Gaz...FCCH | −5.65 | −13.26 | 24.77 | −4.84 | −3.46 |
| α-Cl-Gaz...FCCH | −6.02 | −14.72 | 27.16 | −5.20 | −4.15 |
| α-Br-Gaz...FCCH | −6.16 | −12.23 | 23.70 | −6.47 | −1.76 |

**Figure 4.** Optimized structures of selected dimers. Distances in Å and angles in degs.

accounting for just over half of the total of (ele + pol + disp). The electrostatic component is a bit smaller at 30%, followed by dispersion with just under 20%.

2.3. Substituted Bz

Replacement of the B atom of Bz by its heavier analogues Al and Ga leads to mild strengthening of the interaction with FCCH, as documented in Table 1 and Figure 4. The most strongly bound of this set is Alz, with an interaction energy of 4.4 kcal/mol. This trend is mirrored by the AIM data in Table 2 for all three quantities, ρ , $\nabla^2\rho$, and H. Similar observations apply to the total intermolecular charge transfer and $E^{(2)}$ in Table 3. The components of the interaction energy likewise obey the B < Ga < Al trend, with the exception of the dispersion which is smallest for Al.

Another sort of substitution leaves the B in place but adds halogen atoms at various locations around the ring. These electron-withdrawing agents are expected to amplify the σ -hole on the B atom, and thereby ramp up the interaction energy and its various contributing factors. And indeed, the interaction and binding energies for these species are magnified versus the simple Bz...FCCH complex. The next three rows of Table 1 indicate the largest effect arises for α-F-Bz where the substituent lies adjacent to the B atom, followed by γ and β in that order. The following two rows show that replacing the F substituent by Cl or Br have a similar effect as F, albeit just slightly smaller.

One can similarly add the halogen substituents to the α position of the other rings, which contain either Al or Ga. The placement of F in this position has no effect on Alz, although both Cl and Br do yield a bond strengthening. In the case of the heavier analogue Ga, all three halogen atoms enhance the energetics, more so for Cl and Br than F. Many of these substitutions have comparable effects upon the other manifestations of bonding strength. For example, the AIM parameters are raised by the largest amount when the F substituent is placed in the α position, as are CT and $E^{(2)}$.

With respect to energy partitioning, the values of the ele and pol components are particularly sensitive to the placement of the F substituent on the Bz ring, with the α-substitution having the largest magnifying effect. This quantity is only reduced by a small amount when this F atom is replaced by Cl or Br. With respect to the Alz ring, F-substitution raises the dispersion contribution, with smaller changes in the other terms.

2.4. Addition of Li⁺

One would anticipate that a cation would prefer to situate itself above the phenyl ring where it can benefit from the negative MEP generated by its π-electron system. In this position, the cation ought to suck electron density from the aromatic group, and thus amplify the σ -hole on the Tr atom. This deepened

hole should in turn be able to engage in a stronger triel bond with the FCCH nucleophile.

These premonitions are in fact correct, as may be seen first in Table 5 which documents the rise in V_{\max} near the Tr atom caused by the addition of the Li^+ above the ring, as exemplified by $\text{Li}^+\cdots\alpha\text{-Br-Alz}\cdots\text{FCCH}$ in Figure 5. This σ -hole deepening represents an increase of some 62–85%. The geometric, energetic, and electron density features of the various triads are reported in Table 6. Following each of the Tr bond length R , the interaction energy, the BCP density, and the intermolecular charge transfer are recorded the change in each when compared to the dyad in the absence of the Li^+ . All four quantities reflect the anticipated

strengthening of the Tr bond. The Tr-F distance contracts a good deal, as much as 0.66 Å for $\text{Li}^+\cdots\text{Bz}\cdots\text{FCCH}$. The interaction energies are enhanced by some 55–82%, accompanied by a similar percentage rise in the density at the triel bond critical point, 43–89%. Another perturbing effect of the Li^+ cation is its ability to amplify the amount of charge that is transferred from each nucleophile, in part by acquiring some of this density itself. The last two columns of Table 6 reflect this facilitation of charge transfer, with the total rising between 32 and 80%. It might be noted finally that the positive effects of cooperativity are particularly large for $\text{Tr}=\text{B}$ as compared to the heavier triel atoms.

3. Discussion

One of the unexpected aspects of the trends reported here is the observation that the interaction between Bz and $\text{XC}\equiv\text{CH}$ increases as the X atom grows in size, $\text{F} < \text{Cl} < \text{Br} < \text{I}$. The associated drop in electronegativity might be anticipated to reduce any negative charge on X, and thereby weaken its electrostatic attraction to the σ -hole on B. And indeed, the natural charge on the X atom of HCCX varies in the order $-0.306, +0.119, +0.214, +0.335$ from F to I, so the halogen atom is not even necessarily negatively charged. But it is not the overall charge on the atom that is important as much as the value of V_{\min} in the site which is being approached by the Tr σ -hole. And a glance at Figure 2 shows an opposite pattern that V_{\min} on the X atom of $\text{HC}\equiv\text{CX}$ becomes more negative as X is enlarged so the pattern in interaction energies is not anomalous at all. In order to check as to whether this energetic trend is particular to the B atom, the same complexes were computed with B replaced by Al. Nevertheless, this same order persisted, with interaction energies equaling to 4.41, 9.15, 10.71, and 14.23 kcal/mol for F, Cl, Br, and I, respectively. It might be noted that the magnitude of the rise in interaction energy for each progressive enlargement of X does not quantitatively match the steps in V_{\min} , but the overall pattern is consistent.

In most previously studied triel-bonded complexes, the triel atom usually provides a π -hole to the electron donor. The Trz units examined here differ in a fundamental way in that each Tr atom offers a σ -hole to the nucleophile, so a comparison of σ and π -hole complexes is in order. In the first place the increasing interaction energies of XCCH as X grows larger is also common to the π -hole monomer units BH_2X .^[42] This conclusion is also true for hydrogen bond^[43] and regium bond.^[44] Both electrostatic and orbital interactions contribute to the stronger interaction for the heavier halogen atom.

As another example of the latter, the BH_3 , AlH_3 , and GaH_3 series are each planar units containing a π -hole above the Tr atom. When this hole engages in a TrB with FCCH, the interaction energies for these three Lewis acids are^[45] respectively $-1.11, -2.21, \text{ and } -1.23$ kcal/mol. As listed in Table 1, the same quantity for the σ -holes in Bz, Alz, and Gaz are $-2.15, -4.41, \text{ and } -2.25$ kcal/mol. The order is preserved but these σ -complexes are more strongly bound by a factor of 2.

Table 5. Maximum MEP (V_{\max} , au) on the σ -hole of the Tr atom in the binary complexes with Li^+ and its change (ΔV_{\max} , au) relative to the corresponding monomers.

| | V_{\max} | ΔV_{\max} |
|---|------------|-------------------|
| $\text{Li}^+\cdots\text{Bz}$ | 0.4597 | 0.3897 |
| $\text{Li}^+\cdots\text{Alz}$ | 0.4353 | 0.2695 |
| $\text{Li}^+\cdots\text{Gaz}$ | 0.4407 | 0.3332 |
| $\text{Li}^+\cdots\gamma\text{-F-Bz}$ | 0.4677 | 0.3600 |
| $\text{Li}^+\cdots\beta\text{-F-Bz}$ | 0.4681 | 0.3856 |
| $\text{Li}^+\cdots\alpha\text{-F-Bz}$ | 0.4664 | 0.3796 |
| $\text{Li}^+\cdots\alpha\text{-Cl-Bz}$ | 0.4646 | 0.3535 |
| $\text{Li}^+\cdots\alpha\text{-Br-Bz}$ | 0.4632 | 0.3797 |
| $\text{Li}^+\cdots\alpha\text{-F-Alz}$ | 0.4429 | 0.2845 |
| $\text{Li}^+\cdots\alpha\text{-Cl-Alz}$ | 0.4416 | 0.3141 |
| $\text{Li}^+\cdots\alpha\text{-Br-Alz}$ | 0.4407 | 0.3130 |
| $\text{Li}^+\cdots\alpha\text{-F-Gaz}$ | 0.4471 | 0.3444 |
| $\text{Li}^+\cdots\alpha\text{-Cl-Gaz}$ | 0.4459 | 0.3048 |
| $\text{Li}^+\cdots\alpha\text{-Br-Gaz}$ | 0.4451 | 0.3414 |

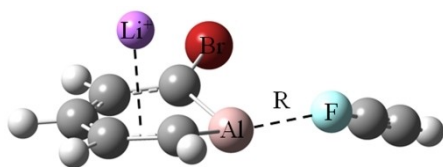


Figure 5. Optimized structure of $\text{Li}^+\cdots\alpha\text{-Br-Alz}\cdots\text{FCCH}$ triad.

Table 6. The $\text{Tr}\cdots\text{X}$ distance (R , Å), interaction energy of triel bond (E_{int} , kcal/mol), electron density (ρ , au) at the $\text{Tr}\cdots\text{X}$ BCP, and NBO charge transferred from nucleophile (CT, e) in the ternary systems and their difference (Δ) relative to the diads.

| | ΔR | E_{int} | ΔE_{int} | $\Delta\rho$ | ΔCT |
|--|------------|------------------|-------------------------|--------------|-------------------|
| $\text{Li}^+\cdots\text{Bz}\cdots\text{FCCH}$ | -0.663 | -11.95 | -9.80 | 0.044 | 0.142 |
| $\text{Li}^+\cdots\text{Alz}\cdots\text{FCCH}$ | -0.195 | -11.36 | -6.95 | 0.015 | 0.029 |
| $\text{Li}^+\cdots\text{Gaz}\cdots\text{FCCH}$ | -0.256 | -6.22 | -3.97 | 0.021 | 0.032 |
| $\text{Li}^+\cdots\gamma\text{-F-Bz}\cdots\text{FCCH}$ | -0.533 | -13.70 | -10.94 | 0.043 | 0.135 |
| $\text{Li}^+\cdots\beta\text{-F-Bz}\cdots\text{FCCH}$ | -0.516 | -13.83 | -11.18 | 0.042 | 0.136 |
| $\text{Li}^+\cdots\alpha\text{-F-Bz}\cdots\text{FCCH}$ | -0.281 | -17.08 | -12.48 | 0.037 | 0.105 |
| $\text{Li}^+\cdots\alpha\text{-Cl-Bz}\cdots\text{FCCH}$ | -0.313 | -16.07 | -11.70 | 0.037 | 0.108 |
| $\text{Li}^+\cdots\alpha\text{-Br-Bz}\cdots\text{FCCH}$ | -0.316 | -15.59 | -11.30 | 0.030 | 0.104 |
| $\text{Li}^+\cdots\alpha\text{-F-Alz}\cdots\text{FCCH}$ | -0.257 | -12.06 | -7.65 | 0.019 | 0.040 |
| $\text{Li}^+\cdots\alpha\text{-Cl-Alz}\cdots\text{FCCH}$ | -0.238 | -12.38 | -7.36 | 0.018 | 0.038 |
| $\text{Li}^+\cdots\alpha\text{-Br-Alz}\cdots\text{FCCH}$ | -0.233 | -12.47 | -7.26 | 0.031 | 0.037 |
| $\text{Li}^+\cdots\alpha\text{-F-Gaz}\cdots\text{FCCH}$ | -0.242 | -6.25 | -3.84 | 0.022 | 0.034 |
| $\text{Li}^+\cdots\alpha\text{-Cl-Gaz}\cdots\text{FCCH}$ | -0.237 | -6.48 | -3.59 | 0.022 | 0.034 |
| $\text{Li}^+\cdots\alpha\text{-Br-Gaz}\cdots\text{FCCH}$ | -0.175 | -6.49 | -3.57 | 0.018 | 0.023 |

Another facet of these TrBs is the effect of halogen substitution on the Lewis acid. In the context of the X-Trz systems examined here, its σ -hole interaction with FCCH is enhanced by halosubstitution. While F has a larger perturbing effect than Br and I for X–Bz, the opposite order is observed for X–Alz and X–Gaz, although it must be added that the differences are rather small in all cases. Again using FCCH as an electron donor for purposes of comparison, its interaction with the π -hole TrX₃ acids is also magnified by the halosubstitution. In terms of the comparison between different X atoms, however, the trends in the π -holes are opposite. Whereas BF₃ forms a weaker complex than do BCl₃ and BBr₃, it is the trichloro and tribromo acids that are weaker for Al and Ga.^[45]

This work has examined the effects of adding a cation to the complex, as well as the substituent effects arising from substitution of halogen atoms at various sites on both the Lewis acid and base. A well designed and rational combination of these two phenomena offers an attractive means of regulating the strength of the triel bond. Combination of these two effects has been previously reported for hydrogen and halogen bonds in FCl \cdots CNH \cdots CNM (M=H, Li, and Na),^[46] where ion-pair hydrogen and halogen bonds are present.

It has been demonstrated that adding CP corrections directly to the geometry optimization procedure has an elongating effect on the H-bonding distance.^[47] Thus it is of interest to consider the effect of these CP corrections upon the intermolecular separations of the σ -hole triel bond and the cation- π interaction. These re-optimized distances are 2.477 Å in Bz \cdots FCCH, 2.261 Å in Alz \cdots FCCH, and 2.620 Å in Gaz \cdots FCCH. These values represent elongations of 0.11, 0.03, and 0.19 Å, respectively, as compared to the uncorrected optimizations. On the other hand, the inclusion of counterpoise has much less effect on the charged systems with the added Li⁺ cation. They introduce no change in the intermolecular distances of Li⁺ \cdots Bz or Li⁺ \cdots Alz, and only a 0.022 Å stretch for Li⁺ \cdots Gaz.

4. Conclusions

The TrB between the modified aromatic Trz and FCCH is generally weak, less than 5 kcal/mol. However, there is a dramatic strengthening effect as the F in FCCH is replaced by heavier X atoms, such that the Bz \cdots ICCH interaction energy is 22 kcal/mol. Mild strengthening effects arise when the B atom of Bz is replaced by the heavier Al and Ga, or when electron-withdrawing halogen atoms are added to the phenyl ring. Most of the interactions are due to nearly equal parts of electrostatic and polarization energies, with dispersion contributions smaller but still appreciable. This pattern is changed a bit for XCCH nucleophiles other than FCCH for which polarization exceeds electrostatic attraction.

Acknowledgements

This work was supported by the National Natural Science Foundation of China (21573188) and by the US National Science Foundation (1954310).

Conflict of Interest

The authors declare no conflict of interest.

Keywords: AIM · cation- π · cooperativity · energy decomposition · substituent effect

- [1] S. J. Grabowski, *ChemPhysChem* **2014**, *15*, 2985–2993.
- [2] W. A. Burns, K. R. Leopold, *J. Am. Chem. Soc.* **1993**, *115*, 11622–11623.
- [3] H. J. Jiao, P. V. R. Schleyer, M. N. Glukhovtsev, J. Chandrasekhar, E. Kraka, *J. Am. Chem. Soc.* **1994**, *116*, 7429–7430.
- [4] S. W. Reeve, W. A. Burns, F. J. Lovas, R. D. Suenram, K. R. Leopold, *J. Phys. Chem.* **1993**, *97*, 10630–10637.
- [5] J. S. Murray, P. Lane, T. Clark, K. E. Riley, P. Politzer, *J. Mol. Model.* **2012**, *18*, 541–548.
- [6] J. S. Murray, P. Lane, P. Politzer, *J. Mol. Model.* **2009**, *15*, 723–729.
- [7] M. D. Esrafilii, P. Mousavian, *Chem. Phys. Lett.* **2017**, *678*, 275–282.
- [8] L. Gao, Y. L. Zeng, X. Y. Zhang, L. P. Meng, *J. Comput. Chem.* **2016**, *37*, 1321–1327.
- [9] J. Grotewold, E. A. Lissi, A. E. Villa, *J. Chem. Soc. A* **1966**, *0*, 1034–1037.
- [10] J. Grotewold, E. A. Lissi, A. E. Villa, *J. Chem. Soc. A* **1966**, *0*, 1038–1041.
- [11] H. Kameo, Y. Baba, S. Sakaki, Y. Tanaka, H. Matsuzaka, *Inorg. Chem.* **2020**, *59*, 4282–4291.
- [12] G. P. McGovern, D. Zhu, A. J. A. Aquino, D. Vidović, M. Findlater, *Inorg. Chem.* **2013**, *52*, 13865–13868.
- [13] S. Bhunya, T. Malakar, G. Ganguly, A. Paul, *ACS Catal.* **2016**, *6*, 11, 7907–7934.
- [14] I. Bhattacharjee, S. Bhunya, A. Paul, *Inorg. Chem.* **2020**, *59*, 1046–1056.
- [15] D. B. Diaz, A. K. Yudin, *Nat. Chem.* **2017**, *9*, 731–742.
- [16] M. D. Esrafilii, F. M. Sabet, *Struct. Chem.* **2016**, *27*, 1157–1164.
- [17] Z. Q. Chi, W. B. Dong, Q. Z. Li, X. Yang, S. Scheiner, S. F. Liu, *Int. J. Quantum Chem.* **2019**, *119*, e25867.
- [18] J. R. Zhang, Y. X. Wei, W. Z. Li, J. B. Cheng, Q. Z. Li, *Appl. Organometal Chem.* **2018**, *32*, e4367.
- [19] S. J. Grabowski, *Struct. Chem.* **2017**, *28*, 1163–1171.
- [20] S. J. Grabowski, *Molecules* **2015**, *20*, 11297.
- [21] S. J. Grabowski, *ChemPhysChem* **2015**, *16*, 1470–1479.
- [22] J. D. Dunitz, R. Taylor, *J. Chem. Edu.* **1997**, *3*, 89–98.
- [23] S. J. Grabowski, *Phys. Chem. Chem. Phys.* **2017**, *19*, 29742–29759.
- [24] S. J. Grabowski, *Coord. Chem. Rev.* **2020**, *407*, 213171.
- [25] Z. F. Xu, Y. Li, *J. Mol. Model.* **2019**, *25*, 219.
- [26] A. Bauzá, X. García-Llinás, A. Frontera, *Chem. Phys. Lett.* **2016**, *666*, 73–78.
- [27] D. L. Fiacco, K. R. Leopold, *J. Phys. Chem. A* **2003**, *107*, 2808–2814.
- [28] Q. J. Tang, Q. Z. Li, *Mol. Phys.* **2015**, *113*, 3809–3814.
- [29] J. R. Zhang, W. Z. Li, J. B. Cheng, Z. B. Liu, Q. Z. Li, *RSC Adv.* **2018**, *8*, 26580–26588.
- [30] M. X. Liu, H. Y. Zhuo, Q. Z. Li, W. Z. Li, J. B. Cheng, *J. Mol. Model.* **2016**, *22*, 10.
- [31] S. Yourdkhani, T. Korona, N. L. Hadipour, *J. Comput. Chem.* **2015**, *36*, 2412–2428.
- [32] M. D. Esrafilii, P. Mousavian, *Mol. Phys.* **2017**, *115*, 2999–3010.
- [33] M. D. Esrafilii, P. Mousavian, *Mol. Phys.* **2018**, *116*, 388–398.
- [34] J. R. Zhang, X. F. Wang, S. F. Liu, J. B. Cheng, W. Z. Li, Q. Z. Li, *Appl. Organomet. Chem.* **2019**, *33*, e4806.
- [35] Gaussian 09 (Revision A.02), M. J. Frisch, G. W. Trucks, H. B. Schlegel, G. E. Scuseria, M. A. Robb, J. R. Cheeseman, G. Scalmani, V. Barone, B. Mennucci, G. A. Petersson, H. Nakatsuji, M. Caricato, X. Li, H. P. Hratchian, A. F. Izmaylov, J. Bloino, G. Zheng, J. L. Sonnenberg, M. Hada, M. Ehara, K. Toyota, R. Fukuda, J. Hasegawa, M. Ishida, T. Nakajima, Y. Honda, O. Kitao, H. Nakai, T. Vreven, J. J. A. Montgomery, J. E. Peralta, F. Ogliaro, M. Bearpark, J. J. Heyd, E. Brothers, K. N. Kudin, V. N. Staroverov,

- R. Kobayashi, J. Normand, K. Raghavachari, A. Rendell, J. C. Burant, S. S. Iyengar, J. Tomasi, M. Cossi, N. Rega, J. M. Millam, M. Klene, J. E. Knox, J. B. Cross, V. Bakken, C. Adamo, J. Jaramillo, R. Gomperts, R. E. Stratmann, O. A. Yazyev, J. Austin, R. Cammi, C. Pomelli, J. W. Ochterski, R. L. Martin, K. Morokuma, V. G. Zakrzewski, G. A. Voth, P. Salvador, J. J. Dannenberg, S. A. Dapprich, D. Daniels, O. Farkas, J. B. Foresman, J. V. Ortiz, J. Cioslowski, D. J. Fox, Gaussian, Inc, Wallingford, CT, **2009**.
- [36] S. F. Boys, F. Bernardi, *Mol. Phys.* **1970**, *19*, 553–556.
- [37] F. A. Bulat, A. Toro-Labbe, T. Brinck, J. S. Murray, P. Politzer, *J. Mol. Model.* **2010**, *16*, 1679–169.
- [38] R. F. W. Bader, AIM2000 Program, v.2.0 .McMaster University, Hamilton, Canada, **2000**.
- [39] A. E. Reed, L. A. Curtiss, F. Weinhold, *Chem. Rev.* **1988**, *88*, 899–926.
- [40] M. W. Schmidt, K. K. Baldrige, J. A. Boatz, S. T. Elbert, M. S. Gordon, J. H. Jensen, S. Koseki, N. Matsunaga, K. A. Nguyen, S. J. Su, *J. Comput. Chem.* **1993**, *14*, 1347–1363.
- [41] P. F. Su, H. Li, *J. Chem. Phys.* **2009**, *131*, 014102.
- [42] A. Bauzá, A. Frontera, *ChemPhysChem.* **2016**, *17*, 3181–3186.
- [43] H. Y. Zhuo, Q. Z. Li, X. L. An, W. Z. Li, J. B. Cheng, *J. Mol. Model.* **2014**, *20*, 2089.
- [44] M. Gao, Q. Z. Li, H. B. Li, W. Z. Li, J. B. Cheng, *RSC Adv.* **2015**, *5*, 12488–12497.
- [45] Q. Q. Yang, Z. Q. Chi, Q. Z. Li, S. Steve, *J. Chem. Phys.* **2020**, *153*, 074304.
- [46] Q. Z. Li, S. M. Ma, X. F. Liu, W. Z. Li, J. B. Cheng, *J. Chem. Phys.* **2012**, *137*, 084314.
- [47] S. Simon, M. Duran, J. J. Dannenberg, *J. Chem. Phys.* **1996**, *105*, 11024–11031.

Manuscript received: November 19, 2020
Revised manuscript received: December 13, 2020
Accepted manuscript online: December 14, 2020
Version of record online: February 8, 2021